Electromagnetic guided mode resonance in dielectric grating affected by transformation of refractive index periodicity

A. Abramov[1], Y. Yue[1], and V. Rumyantsev[2]
[1]Institute of Deep Perception Technology, Jinghui East Road 90, 214000 Wuxi, China
[2]Galkin Institute for Physics and Engineering, R.Luxemburg 72, 83114 Donetsk, Ukraine

Corresponding author: Y.Yue (e-mail: yueyutao@idpt.org).

ABSTRACT The present work studied effects of transformation of refractive index periodicity on electromagnetic wave propagation through grating waveguides. In lieu of the standard refractive index periodicity, although its unit cell consists of two kinds of materials, we consider few such unit cells as a new supercell, where the material parameters in a standard unit cell are changed. It has been shown how by changing parameters of the periodicity to control the wavelength and intensity of resonant optical mode (guided mode resonance) arising inside grating area. High quality factor calculated for the specific angle of incidence and periodicity parameter. Thus, we demonstrated that transformation of refractive index provides additional tools of controlling the GMR, and that means the sample can be designed more functional in terms of real application.

INDEX TERMS Electromagnetic wave, grating, refractive index, resonance.

I. INTRODUCTION

THIN layers containing a periodic variation of the refractive index along the layer have attracted considerable interest in photonics because of their significant role in applications such as filters [1], sensors [2], lasers [3], etc. and in several diverse areas, such as acousto-optics [4], integrated optics [5], holography [6], and spectroscopy [7]. The periodic variation is usually obtained by means of a dielectric grating, which is superimposed on the upper surface of a substrate configuration. Although the diffraction of electromagnetic waves by planar gratings has been extensively studied for decades, the development of new technologies in sample growth and the means of their study have renewed considerable interest in these structures in recent years. A surface diffraction two-dimensional (2D) grating structure placed on the topmost layer of distributed Bragg reflectors was exploited as sample for biosensing applications [8]. All-dielectric quasi–three-dimensional subwavelength structure, consisting of multilayer films and metagratings, to achieve perfect anomalous reflections at optical frequencies has been proposed in [9]. A potential application of diffraction grating in optical sensing and imaging from visible to near-IR wavelengths have been demonstrated in [10]. New effects in grating structures can also be found due to the presence of material components with specific properties. In [11] authors demonstrated a grating-graphene metamaterial where grating-induced field enhancement significantly increases the already large THz nonlinearity of graphene, which allows the creation of higher harmonics (up to the ninth). A tunable graphene-based lattice structure has been proposed as the building blocks of several infrared systems in [12].

The operation of devices containing a dielectric grating depends on the properties of the electromagnetic fields guided by the structure. These fields appear either as surface waves traveling parallel to the structure or as leaky waves guided by the structure. Both types of waves appear as characteristic (free resonant) solutions of the boundary-value problem prescribed by the layer configurations. For specific combinations of incident angle and optical frequency, a resonance exists that allows the grating to couple light into a guided mode of the waveguide. For this guided mode resonance (GMR), the normally transparent structure becomes reflective. If the grating period is sub-wavelength, then the normally transparent structure becomes a mirror under resonance conditions. At resonance, the intensity in the waveguide region is also much higher.

The reviews published in recent years [13, 14] confirm the importance of GMR in broad range of applications in research and industry. In particular, GMR gratings have been implemented in photodetectors [15], spectrometers [16], switching devices [17], sensors [18]. Let us also mention that most of the known resonant effects arising in optics and photonics can be investigated by studying diffraction gratings. For instance, the vast majority of the published

papers studying photonic bound states in continuum focus on gratings and other periodic structures [19].

Therefore, a thorough study of GMR's origin, features and various factors affecting them is of great theoretical and practical importance. In the present work, we have investigated how changes in refractive index periodicity in the grating area affect the intensity and wavelength of GMRs. The conditions for an high quality factor have been discussed. We have demonstrated that the grating can be designed to offer more functionality by changing the specific parameters of the grating structure.

II. RIGOROUS COUPLED-WAVE ANALYSIS FOR PLANAR DIFFRACTION

To analyze the diffraction of electromagnetic waves by spatially modulated media, we use the most common Rigorous Coupled-Wave Analysis [20]. There are many other approaches for the investigation of the diffraction by grating structures: the coordinate-transformation-based differential [21] for modeling surface-relief gratings; a modified method of lines [22] can accurately calculate not only average power but also field and phase distribution across reflected waves for apodised fibre gratings; rigorous integral equation method [23] combines semianalytical techniques and the Method of Moments exhibiting superior accuracy and numerical efficiency compared to other methods. The RCWA are well developed and validated [13, 19, 20] especially for the types of structure we studied in our work. Another advantage of the method is a clear physical insight and a simple way to directly recover all the results we present.

The goal is to find solutions of Maxwell's equations in and out of the grating regions and then to match the tangential electric and magnetic field components at the boundaries. In the case of planar diffraction, the incident electric field is normal to the plane of incidence and all diffracted orders (forward and backward) lie in the same plane (the plane of incidence, the $x-z$ plane, (Fig.1)).

Let us briefly describe the rigorous coupled-wave analysis that we use in our calculations. Here we refer to Ref. [20], where a full description of the method can be found. The incident TE polarized and normalized electric field impinges on the grating structure at an angle θ (Fig. 1), given by

$$\vec{E}_{\mathrm{inc},y}(\vec{r}) = \exp(-i(k_{\mathrm{x}0}x + k_{z0}z)) \qquad (1)$$

where k_{x0} and k_{z0} are x- and z- components of the incident light wave vector. The normalized solutions in region I ($z<0$) and in region II ($z>d$) are given by

$$E_{\mathrm{I},y}(\vec{r}) = E_{\mathrm{inc},y} + \sum_i R_i \exp(-i(k_{xi}x + k_{I,zi}z)) \qquad (2)$$

$$E_{\mathrm{II},y}(\vec{r}) = \sum_i T_i \exp(-i(k_{xi}x + k_{II,zi}(z-d))) \qquad (3)$$

where k_{xi} is given by

$$k_{xi} = k_{x0} - i2\pi/L \qquad (4)$$

and

$$k_{l,zi} = \begin{cases} +\sqrt{(k_0 n_l)^2 - k_{xi}^2} & k_0 n_l > k_{xi} \\ -i\sqrt{k_{xi}^2 - (k_0 n_l)^2} & k_{xi} > k_0 n_l \end{cases} \qquad (5)$$

$L=I,II$, $k_0 = 2\pi/\lambda_0$ and λ_0 is the wavelength of light in free space, R_i is the normalized electric-field amplitude of the i th backward-diffracted (reflected) wave in region I, T_i is the normalized electric-field amplitude of the forward-diffracted (transmitted) wave in region II, and n_l is the refractive index in the appropriate region. The magnetic fields in regions I and II can be obtained from Maxwell's equation

$$H = \frac{i}{\omega\mu}\nabla \times E \qquad (6)$$

where μ is the permeability of the region and ω is the angular optical frequency.

In the grating region ($0 < z < d$) the tangential electric (y-component) and magnetic (x–component) fields can be expressed by a Fourier expansion in terms of space-harmonic fields as

$$E_{\mathrm{g}y} = \sum_i S_{yi}(z)\exp(-ik_{xi}x) \qquad (7)$$

$$H_{\mathrm{g}x} = -i\left(\frac{\varepsilon_0}{\mu_0}\right)^{1/2}\sum_i U_{xi}(z)\exp(-ik_{xi}x) \qquad (8)$$

where ε_0 and μ_0 are the permittivity and permeability of free space, respectively. $S_{yi}(z)$ and $U_{xi}(z)$ are the normalized amplitudes of the ith space-harmonic fields.

Substititing E_{gy} and H_{gx} into Maxwell's equation for the grating region we obtain eigenvalue problem for $S_{yi}(z)$. Its solutions w_{im} (eigenvector) and q_m (eigenvalue) are used to form general expression for the fields in the grating region.

Since waves can travel along the positive and negative directions of the z axis within the grating area, the dependence on z can be expressed as

$$S_{yi}(z) = \sum_m w_{i,m}\left(\mathrm{c}_m^+ \exp(-k_0 q_m z) + \mathrm{c}_m^- \exp(k_0 q_m (z-d))\right)$$

$$U_{xi}(z)=\sum_m v_{i,m}\left(-\mathrm{c}_m^+\exp(-k_0q_mz)+\mathrm{c}_m^-\exp(k_0q_m(z-d))\right)$$

where $v_{im}=q_mw_{im}$, c_m^+ and c_m^- are unknown constants. Using the boundary conditions we arrive at a system of linear equations with unknown coefficients: R, T, c^+, c^-.

Let us bring two final equations for unknown c^+ and c^-:

$$\mathrm{c}^+ - Rg_I\mathrm{c}^- = A_{inc} \tag{9}$$

$$\mathrm{c}^- - Rg_{II}\mathrm{c}^+ = 0 \tag{10}$$

where A_{inc} is equal to amplitude of the incident field, and $R_{gI,II}=(v+k_{I,II}w)^{-1}(v-k_{I,II}w)\exp(-k_0qd)$, w and v are the matrixes appeared in (11) and (12). Actually, $Rg_{I,II}$ are also matrixes, which act as reflection operators within the grating area. Indeed, it can be seen from (13-14) that Rg_I acts on c^- and, after adding the incident field, forms the amplitude of the field (c^+) propagating in the opposite direction. Rg_{II} acting on c^+ also forms the amplitude of the field (c^-) propagating in the opposite direction. In the absence of the incident field, the system of equations (13-14) only has a solution when the next determinant vanishes, that is:

$$F(k_{x0},k_0)=det(1-Rg_IRg_{II})=0 \tag{11}$$

It is dispersion relation for the GMRs.

III. DESIGN AND PARAMETERS OF THE GRATING STRUCTURE

The structure that we use in our simulations is depicted in Fig. 1. We consider plane wave incidence from air to a grating structure superimposed on a substrate made of SiO_2 with a refractive index of 1.47. For TE-polarized light, the incident plane wave is perpendicular ($\theta = 0°$) and the electric field is parallel to the y axis. The grating consists of alternating high/low-index dielectric bars. The refractive indices of the high/low-index bars are taken as n_1 =3.44 and n_2 = 1.0, which represent the values of *Si* and air, and their widths are fixed at d_1 and d_2, with $L=d_1+d_2$ being the length of the standard unit cell, and d its thickness. We then combine these three unit cells (N_c=3) into a new unit cell, where one Si bar is removed. The case of Nc =5 is also considered in this paper. Schematic representation of the refractive index profile for Nc =1, 3, 5 is shown in Fig.2. We kept the length $L=0.5$ and $d=0.5$ constant in all our calculations. All sizes and lengths are given in μm. SiO_2 and *Si* have been chosen as the main materials for the structure because of the importance of *Si* in modern optical materials.

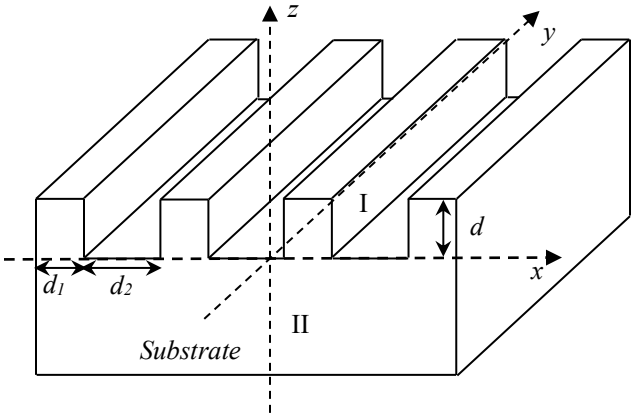

FIGURE 1. Grating structure. The outer substrate is extended to infinity.

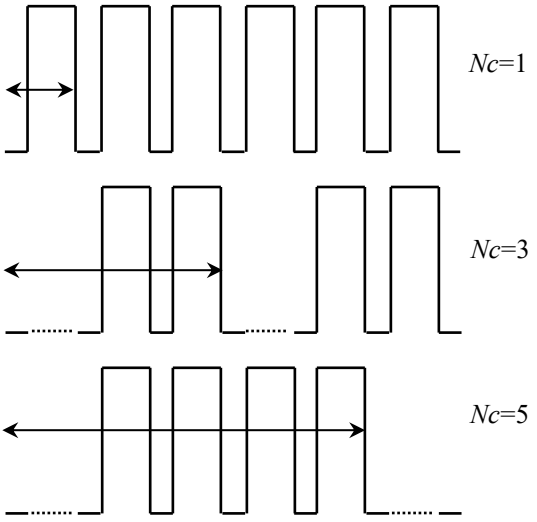

FIGURE 2. Schematic view of the refractive index for different values of number of standard unit cells Nc. Line with arrows show an unit cell.

Also this combination of materials is often found as the main materials from which the grating is made [24-25].

IV. GUIDED-MODE RESONANCES

In periodic structures similar to those studied in this work, the so-called anomalous reflection can manifest itself [26]. It is associated with multiple diffraction orders. The main contribution to the reflected/transmitted wave comes from several modes (several initial values of |m| in expansion (2,3)). The anomaly lies in the discrepancy between the reflection angle and the predicted Snell's law. The latter corresponds to the dominant contribution to the amplitude of the term with m = 0, while in such structures the main contribution comes from the terms with $|m|>0$. However, the purpose of this work is to analyze resonances in the reflection/transmission spectra of waves, regardless of the direction of their propagation, so the analysis of the contributions of the modes is not essential here, and may be the subject of a special study.

In this section, we study how the angle of incident plane wave and the parameters of the structure affect the wavelength and intensity of the GMR's. For that, we consider the dispersion relation for the GMRs (11). Generally it consists of two parameters k_0 and k_{x0}. We consider here its solutions within the so-called light cone when using the standard relation: $k_{x0}=k_0 \sin(\theta)$. Thus varying the angle of incidence, we can calculate the position of the guided mode resonance (the value k_0, which uniquely corresponds to the wavelength of the incident light) for different angles. Since the function $F(k_{x0},k_0)$ in (15) has complex values, we find numerically its real and imaginary parts in a certain wavelength range, and then we can choose such a value λ_r for which $Re(F) \approx 0$ and $Im(F) \approx 0$. For better visualization we also focused on the value of $1/|F|$. An example is shown on Figure 3. Note that if for some value of wavelength the values of $Re(F)$ or $Im(F)$ are close to zero then also the sharp peaks could be arise on the dependencies (for λ =3.0 on Fig.3), but they are not relating to the GMR, because the corresponding value of wavelength are not solution of equation (11).

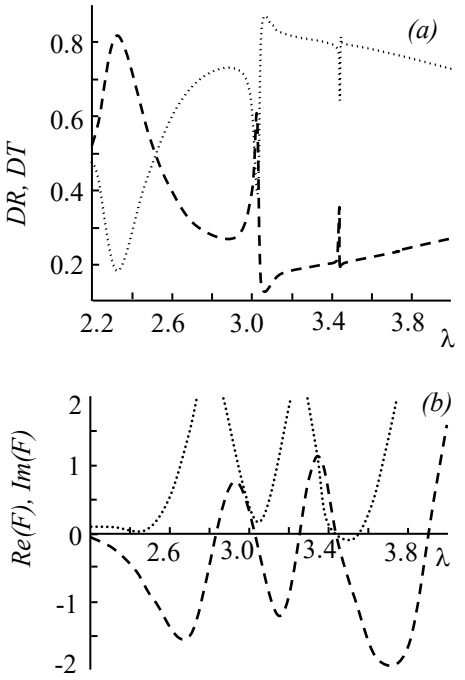

FIGURE 3. The diffraction efficiencies of the transmitted (dashed line) and reflected (dots) waves (a), and Real (dashed line) and Imaginary (dots) parts of function F versus wavelength (b); Nc=5, θ=45°, d_1/L=0.6.

Having calculated the field amplitudes R and T, and the formulas given in [27], it is easy to calculate the diffraction efficiencies of the transmitted DT and reflected DR waves. These quantities are integral characteristics used to estimate the scattered energy. For the same range of the wavelengths, the dependencies of the real and imaginary parts of the function F are presented.

It can be clearly seen that the zero of the function F corresponds to the resonance position at $\lambda_r=3.4$. To explain the origin of that resonance we have to note first we are considering the case of Nc =5. This means that 5 standard cells are merged into one supercell. Meanwhile, the parameters of one of the materials have changed. Thus, we can consider this supercell as a periodic structure with a defect. When light passes through such a structure, the frequency dependence of transmission and reflection is characterized by a pronounced resonance in the form of a narrow peak [28, 29]. To define the position of this kind of resonance, we calculated the frequency band structure of a 1D photonic crystal with the cell described above (as a supercell in the case of Nc=5). The presence of defect frequencies is expected in the form of narrow bands with small dispersion. However, in the grating structure, the wave vector has two components, while the defect frequency λ_{1D}^{def} was calculated for the purely 1D case. That is why there is no exact match between λ_{1D}^{def} and λ_r. But there is a simple way to bind these two values. For instance, for incidence angle of 45º we have $k_x=k_z=k_0\sqrt{2}$. Assuming that k_x corresponds wave propagation along periodicity direction, while k_0 – to the resonant wavelength, we have

$$\lambda_r = \lambda_{1D}^{def} / \sqrt{2} \qquad (12)$$

Indeed, for d_1/L=0.6 relation (12) is true as $\lambda_r=3.4$ (Fig.3) and $\lambda_{1D}^{def} \approx 4.8$ (calculated 1D band structure) and just the case has been calculated on Fig.3. Thus, a sharp peak in the values of DR and DT at the resonant wavelength is corresponding to the characteristic defect frequency.

We also varied the ratio of d_1/L to investigate its effect

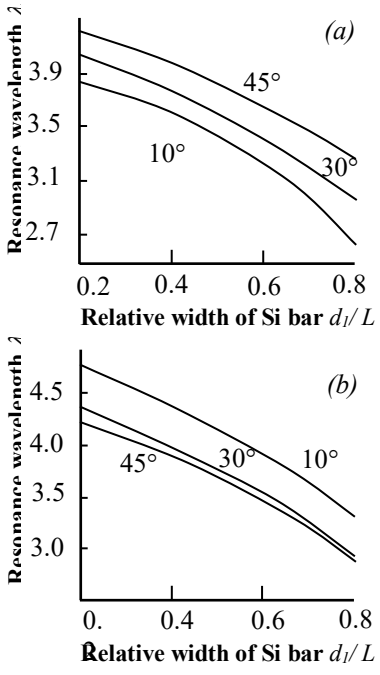

FIGURE 4. Resonance wavelength for different incidence angles. (*a*) - Nc=3; (*b*) - Nc=5.

on GMR positions. The corresponding results are presented in Fig. 4 for *Nc=3 and 5*. The values for the dependencies on Figures 4,5 were obtained according to the procedure described above: the resonant wavelength has been calculated as solution of equation (11) for a given angle of incidence and a width d_1 of Si grating. Let us consider its two main features: for any line and any angle of incidence, the value of the resonant wavelength decreases as the ratio d_1/L increases (*i*); for a fixed value of the ratio d_1/L, the resonant wavelength increases as the angle of incidence increases with *Nc=3* and vice versa for *Nc=5* (*ii*). Both of these features can be explained through a simple theory described in Ref. [30]. According to [30], the resonance regimes are defined by the following inequalities:

$$max(n_I,n_{II}) \le |n_I \sin(\theta)-i\lambda/L| < n_g$$

Here, n_g is the average value of the refractive index in grating area. After [31] it can be calculated by the formula:

$$n_g = \sqrt{n_1^2 + f(n_2^2 - n_1^2)}$$

where $n_{1,2}$ are the refractive indexes of the materials within the unit cell, and *f* is given by the areas covered by n_2 over the period. Thus, it is easy to calculate appropriate values for *Nc=3* and *Nc=5*. Moreover, it turns out that these values depend on the ratio *d1/L*, in such a way that as this ratio increases, n_g decreases. Therefore, increasing the ratio *d1/L* leads to a shift of resonant wavelengths towards smaller quantities. On the other hand, the angular dependence of the resonant wavelength has the opposite character of change for different λ/L ratios (see a typical figure in [30]), which leads to the different angular dependences of the resonances for *Nc=3* and *Nc=5*.

Assuming the above, it can be concluded that the grating couples light into the guided mode for specific combinations of incident angle, light wavelength, different material fractions (ratio d_1/L) and refractive index periodicity of the unit cell structure.

At resonance, a structure becomes reflective and has a much higher intensity in the grating region. For *Nc=3 (a)* and *Nc=5 (b)*, the dependence of the field intensity within the grating area on the resonant wavelength is shown in Fig. 5. Despite the absence of a correlation between the dependencies for these cases, their behavior can be explained by the same factor: the frequency band structure of the 1D periodic sample. The case *Nc =3* corresponds to a regular periodic structure: its frequency band structure consists of dispersion curves separated by gaps and is the same for each d_1/L value. By increasing the angle of incidence, we shift the resonance position, thus moving it away from the allowed frequency band. This shift leads to a decrease in field intensity. If we consider the intensity values for each separate incident angle value, then their

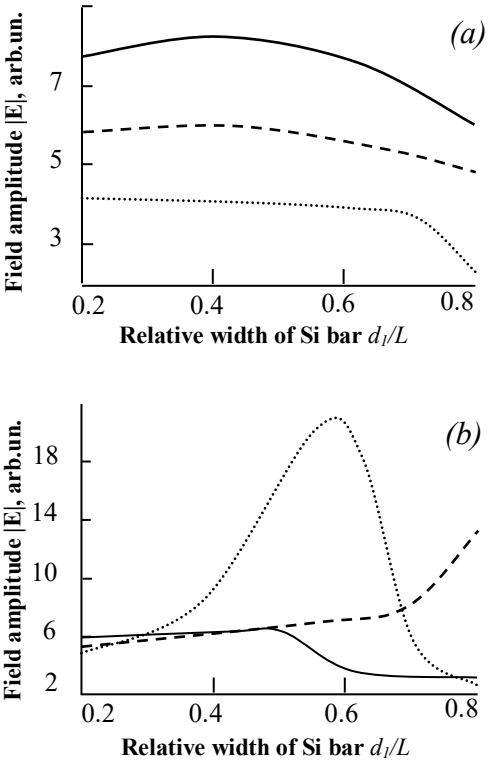

FIGURE 5. Field amplitude at GMRs for incidence angles: solid - 10°; dashed - 30°; dots - 45°; a – *Nc*=3; b – *Nc*=5. The values for 45° (b) are halved.

quantities also depend on the position of the resonances with respect to the nearest frequency band: if they are approaching that band, then the intensity can even be increased (as for line 1 and partly for line 2), while in the case of line 3 it can be concluded that the resonance moves away from the band.

The absence of a clear regularity of the lines in Fig. 5(b) is attributed to the existence of defect lines in the frequency band structure of the 1D sample for *Nc*=5. If GMR appears in the vicinity of the defect frequencies (corresponding to 1D samples according a relation (12)), then their proximity to them leads to a sharp increase in intensity. Otherwise, we

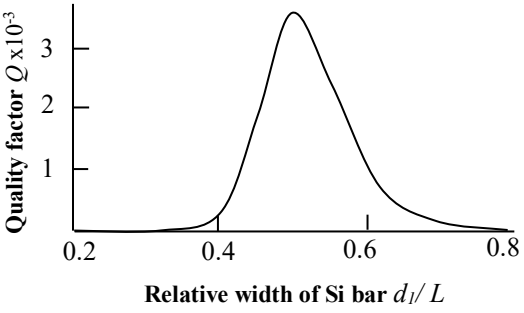

FIGURE 6. Quality factor *Q*: *Nc=5, θ=45°*.

see smooth changes in intensity (as in lines (1-3) in Fig. 5).

For the case of maximum intensity $Nc=5$ and $\theta=45°$, we calculated the corresponding quality factors (Fig. 6).

As we mentioned above, this high value can be really explained by the correspondence of the resonance position with the defect frequency of the 1D periodic sample.

Generally, waves propagating in the grating area have two practically independent eigenmodes: transverse (along the z axis) and longitudinal (along the direction of periodicity). Besides, if the eigenvalues of these modes are very close to each other, then this leads to an increase in intensity. Therefore, by combining structural parameters (periodic elements, thickness) and incident waves (angle, wavelength), it is possible to design samples for specific purposes.

Thus, a sharp peak in the values of DR and DT at the resonant wavelength coincides with the characteristic defect frequency.

V. CONCLUSION

In conclusion, we consider the planar diffraction of electromagnetic waves through silicon-on-insulator grating waveguides. By introducing complex unit cells of refractive index periodicity into the grating area, extra states known as guided mode resonances can be created. In order to study its effect on GMR positions, the variation of periodicity parameters has been considered. The results show that a wavelength shift of the GMR and a deformation of the diffraction efficiency spectrum exist with changes in ratio of different material fractions as well as with different angles of the incident field. The wavelength shift of GMR correlates with the frequency band structure caused by the 1D periodicity of the refractive index. The GMRs are very sensitive to changes in different periodicity parameters. In particular, it is found that by varying the grating parameters, it is possible to match the eigenmodes along and across the structure in such a way that an extremely large value of the quality factor can be obtained. Thus, the grating can be designed to achieve strong wavelength-dependent behavior and/or high local field intensities.

REFERENCES

[1] S Tibuleac, R. Magnusson, "Reflection and transmission guided mode resonance filters," J. Opt. Soc. Am A, vol. 14, no.7, pp. 1617 – 1626, 1997, 10.1364/JOSAA.14.001617.

[2] L. Davoine, et al. "Resonant absorption of a chemically sensitive layer based on waveguide gratings," Appl Opt, vol. 52, no. 3, pp. 340– 349, 2013, 10.1364/AO.52.000340.

[3] M. Wang, Q. Guo, S. Wang, et al., "Interference femtosecond laser stamping of micro-grating structures and time-resolved observation of its dynamics," Opt. Express, vol. 28, no. 12, pp. 18376-18386, 2020, 10.1364/OE.390012.

[4] A. Xie, F. Song, S-W. Seo, "An acousto-optic sensor based on resonance grating waveguide structure," Sensors and Actuators A: Physical, vol. 216, pp. 364–369, 2014, 10.1016/j.sna.2014.06.012.

[5] B.E. Little, S.T. Chu, W. Pan, Y. Kokubun, "Microring resonator arrays for VLSI photonics," IEEE Photonics Technology Lett., vol.12, no. 3, pp. 323–325, 2000, 10.1109/68.826928.

[6] F. Havermeyer, W. Liu, C. Moser, D. Psaltis, G. Steckman, "Volume holographic grating-based continuously tunable optical filter," Optical Engineering, vol. 43, pp. 2017-2021, 2004, 10.1109/JSTQE.2007.896060.

[7] T. Rasmussen, "Overview of High-Efficiency Transmission Gratings for Molecular Spectroscopy," Spectroscopy, vol. 29, pp. 32-39, 2014.

[8] D. Ge, J. Shi, A. Rezk, C. Ma, L. Zhang, P. Yang and S. Zhu, "Two-Dimensional Hole-Array Grating-Coupling-Based Excitation of Bloch Surface Waves for Highly Sensitive Biosensing," Nanoscale Research Lett., vol. 14, pp.:319:1-9, 2019, 10.1186/s11671-019-3159-8.

[9] T. He, T; Liu, S. Xiao, Z. Wei, Z. Wang, L. Zhou, X. Cheng, "Perfect anomalous reflectors at optical frequencies," Sci. Adv. vol. 8, no. 9), pp.1-9, 2022, 10.1126/sciadv.abk3381.

[10] W Li, J Liu, G Cheng, Q Huang, R Zheng, X Wu, "Diffraction gratings based on a multilayer silicon nitride waveguide with high upward efficiency and large effective length," Applied Optics, vol. 61, no. 10, pp. 2604-2609,2022, 10.1364/AO.452651.

[11] J-C. Deinert, D. Iranzo, R. Pérez, X. Jia, etc., "Grating-Graphene Metamaterial as a Platform for Terahertz Nonlinear Photonics." ACS Nano, no. 15, pp. 1145−1154, 2021, 10.1021/acsnano.0c08106.

[12] S. Patel, M. Ladumor, V. Sorathiya, T. Guo, "Graphene based tunable grating structure," Materials Research Express, vol.6, no. 2, pp. 025602, 2018, 10.1088/2053-1591/aaea9a.

[13] G. Quaranta, G. Basset, O. Martin, B. Gallinet, "Recent Advances in Resonant Waveguide Gratings," Laser Photonics Rev., vol. 1800017, pp. 1-31, 2018, 10.1002/lpor.201800017.

[14] F Gambino, M Giaquinto, A Ricciardi, A Cusano, "A review on dielectric resonant gratings: Mitigation of finite size and Gaussian beam size effects," Results in Optics, vol. 6, pp. 100210: 1-19, 2022, 10.1016/j.rio.2021.100210.

[15] A. Zhu, S. Zhu, G-Q. Lo, "Guided mode resonance enabled ultra-compact germanium photodetector for 1.55 μm detection," Opt. Expr., vol. 22, no. 3, pp. 2247–2258, 2014, 10.1364/OE.22.002247.

[16] Y. Hung, C. Kao, T. Kao, C. Huang, J. Lin, C. Yin, "Optical spectrometer based on continuously-chirped guided mode resonance filter," Opt. Express, vol. 26, no. 21, pp. 27515–27527, 2018, 10.1364/OE.26.027515.

[17] Y. Qing, H. Ma, Y. Ren, S. Yu, T. Cui, "Near-infrared absorption-induced switching effect via guided mode resonances in a graphene-based metamaterial," Opt. Express, vol. 27, no. 4, pp. 5253–5263, 2019, 10.1364/OE.27.005253.

[18] Y. Zhou, Z. Guo, W. Zhou, S. Li, Z. Liu, X. Zhao, X Wu, "High-Q guided mode resonance sensors based on shallow sub-wavelength grating structures," Nanotechnology, vol. 31, pp. 325501, 2020, 10.1088/1361-6528/ab8cf0.

[19] D. Bykov, E. Bezus, L. Doskolovich, "Coupled-wave formalism for bound states in the continuum in guided-mode resonant gratings," Phys. Rev A, vol. 99, pp. 063805, 2019, 0.1103/PhysRevA.99.063805.

[20] M.G. Moharam, E.B. Grann, D.A. Pommet, T.K. Gaylord, "Formulation for stable and efficient implementation of the rigorous coupled-wave analysis of binary gratings," J Opt Soc Am A. vol. 12, pp. 1068-1076, 1995, 10.1364/JOSAA.12.001068.

[21] L. Li, J. Chandezon, G. Granet, J-P. Plumey, "Rigorous and efficient grating-analysis method made easy for optical engineers", Applied Optics, vol. 38, no. 2 pp. 304-313, 1999, 10.1364/AO.38.000304

[22] I. A. Goncharenko, N. Zevras, "Analysis method for apodised grating structures", Optical and Quantum Electronics, vol. 34, pp. 471–479, 2002, 10.1007/BF02892611

[23] N. Tsitsas, Efficient integral equation modeling of scattering by a gradient dielectric metasurface, EPJ Appl. Metamat., vol. 4, no. 3, pp. 1-13, 2017, 10.1051/epjam/2016014

[24] J. Foley, A. Itsuno, T. Das, S. Velicu, J. Phillips, "Broadband long-wavelength infrared Si/SiO2 subwavelength grating reflector," Opt Lett, vol. 37, no. 9), pp. 1523-1525, 2012, 10.1364/OL.37.001523.

[25] M. Asaduzzaman, M. Bakaul, S. Skafidas, M. Khandokar, "Multiple layers of silicon–silica (Si–SiO2) pair onto silicon substrate towards highly efficient, wideband silicon photonic grating coupler," Optical and Quantum Electronics, no. 48, pp.1-13, 2016, 10.1007/s11082-016-0746-0.

[26] N. Tsitsas and C. Valagiannopoulos, “Anomalous reflection of visible light by all-dielectric gradient metasurfaces”, JOSA B, vol. 34, no.7, pp. D1-08, 10.1364/JOSAB.34.0000D1
[27] T. Gaylord, M. Moharam, “Analysis and Applications of Optical Diffraction by Gratings,” Proceedings of the IEEE, vol. 73, no. 5, pp. 894-937, 1985, 10.1109/proc.1985.13220.
[28] A Abramov, L Luan, “Effect of a Gradient Dielectric Permittivity Layer on Optical Properties of a 1D Anisotropic Photonic Crystal,” Journal of Nanoengin. and Nanomanuf., vol. 6, pp. 1– 6, 2016, 10.1166/JNAN.2016.1269.
[29] V.V. Rumyantsev, S.A. Fedorov, K.V. Gumennyk, M.V. Sychanova, “Dispersion characteristics of electromagnetic excitations in a disordered one-dimensional lattice of coupled microresonators,” Physica B, vol. 461, pp. 32– 37, 2015, 10.1016/j.physb.2014.12.009.
[30] S.S. Wang and R. Magnusson, “Theory and applications of guided-mode resonance filters,” Appl Opt., vol. 32, pp. 2606-2613, 1993, 10.1364/AO.32.002606.
[31] J.H. Schmid, P. Cheben, P.J. Bock, et al., “Refractive index engineering with subwavelength gratings in silicon microphotonic waveguides,” IEEE Photonics, vol. 3, pp. 597 – 607, 2011, 10.1364/OL.35.002526.